Research Article

Journal of Labelled Compounds and Radiopharmaceuticals

Received 26 October 2007, Accepted 15 November 2007 Published online 3 January 2008 in Wiley Interscience

(www.interscience.wiley.com) DOI: 10.1002/jlcr.1487

# Possible mechanisms of controlling the configuration, stability, and lipophilicity of [$^{99m}$TcO]$N_3S$ and [ReO]$N_3S$ chelates

Zifen Su,[a]* and Yong Xu[b]

**The relationship of structural characters of the tripeptidic amine–bisamido-thiol ($N_3S$ type) chelators with the lipophilicity, configuration, and stability of four [$^{99m}$TcO]$N_3S$ and one [ReO]$N_3S$ chelates is studied here. The results show that the hydroxymethyl group on the two $N_3S$ chelators, RP294 and RP435, has inhibited neither the formation nor interconversion of *syn* and *anti* stereoisomers of the chelates, while the *tert*-butyl group on RP455 and RP535 has prevented the *anti* isomer from converting to the *syn* one both in acidic and neutral solutions. The interconversion rates of a stereoisomer can be accelerated at higher pH. [$^{99m}$TcO]RP455 is stable in pH 7.4 aqueous solution, while [$^{99m}$TcO]RP535 undergoes decomposition at the same medium, suggesting the influence of a larger side-chain on the stability of the chelate. Unlike [$^{99m}$TcO]RP535, [ReO]RP535 is stable even in 0.1 N NaOH for 3 h without change. Combining factors of medium pH values, nature of substituents on a chelator's backbone, size of side-chains, and property of central metal ions together determine the lipophilicity, configuration, and stability of [$^{99m}$TcO]$N_3S$ and [ReO]$N_3S$ chelates. This information may be useful for a further design of [$^{99m}$TcO]$N_3S$ or [$^{186}$ReO]$N_3S$ or [$^{188}$ReO]$N_3S$ chelates with predictable physicochemical properties favorable for the quality diagnosis of cancers.**

**Keywords:** configurations; $N_3S$ chelator; stereoisomers; [$^{99m}$TcO]$N_3S$ chelate; [ReO]$N_3S$ chelate

## Introduction

Reduction of Na[$^{99m}$$TcO_4$] by $SnCl_2$ usually yields $^{99m}TcO^{3+}$ ion, which can be stabilized and neutralized by tetradentate chelators such as L,L-ethylenedicysteine (where $^{99m}$Tc is coordinated by two nitrogen and two sulfur atoms, $N_2S_2$-type chelator),[1,2] mercaptoacetylglycylglycylglycine ($N_3S$ type),[3] hexamethyl propylene amine oxime ($N_4$ type),[4,5] and ethyl cysteinate dimer ($N_2S_2$).[6,7] Those chelates exhibit a distorted square pyramidal geometry and theoretically exist *syn* and *anti* stereoisomers, depending on the orientation of the backbone substitutions with respect to the metal–oxo bond. Commonly, bio-reactive groups are placed on a chelator backbone or conjugated to a side-chain of the chelator towards improving the target selectivity of the radiochelate. For example, by attaching a 2-nitroimidazole (2NI) group to the chelator of propyleneamine oxime ($N_4$ type), the $^{99m}$Tc chelates (BMS181321 and BRU59-21) have exhibited selective accumulation in hypoxic cells, suggesting the potential for tumor hypoxia imaging.[8–10] Another example is TRODAT, a dopamine transporter-specific imaging agent, which is a $^{99m}$Tc–$N_2S_2$ chelate with a tropane derivative connected to the backbone.[11] Experiences often suggest that conjugating a bio-selective group to a radiolabel does not guarantee a significant improvement of molecule in target selectivity. Specific accumulation of a radiolabel to the target tissue depends on many factors including its physicochemical properties such as structure, configuration, stability, lipophilicity, etc.[12–16] However, a systematic investigation of structure–activity relationships of [MO]$N_2S_2$ or [MO]$N_4$ (where M represents $^{99m}$Tc and Re) radiohelates can be difficult due to the complication in chemical synthesis of bifunctional chelators. This has promoted the application of peptidic bifunctional chelating agents because of the ease in design and preparation by means of solid-phase synthesis.[17–21]

In our previous study on peptidic $N_3S$ chelators for $^{99m}$Tc and Re,[22] it has been noticed that the hydroxymethyl and *t*-Bu groups on the backbone of the chelators played different roles in influencing the stereoisomerization and stability of [$^{99m}$TcO]$N_3S$ chelates. The *syn* and *anti* stereoiosmers of the [$^{99m}$TcO]$N_3S$ chelates with hydroxymethyl group on the chelators were detected by reversed-phase high-performance liquid chromatography (HPLC) but not identified. Unlike the hydroxymethyl group, the *t*-Bu group on the chelators had forced the [$^{99m}$TcO]$N_3S$ chelate to take one preferential configuration. In order to understand the link of the structure of an $N_3S$ chelator and physicochemical properties of the [MO]$N_3S$ chelates, four $N_3S$ chelators with hydroxymethyl and *t*-Bu groups on their backbone and different sizes of side-chains (Figure 1), dimethylglycyl-L-seryl-L-cysteinylglycinamide (RP294),

[a]*Key Laboratory of Radiation Physics and Technology of Ministry of Education of China, Institute of Nuclear Science and Technology, Sichuan University, Chengdu 610064, China*

[b]*State Key Laboratory of Biotherapy, College of Life Science, Sichuan University, Chengdu 610041, China*

**Correspondence to: Zifen Su, Institute of Nuclear Science and Technology, Sichuan University, Chengdu, Sichuan 610064, China.*
*E-mail: zfsu@yahoo.com*

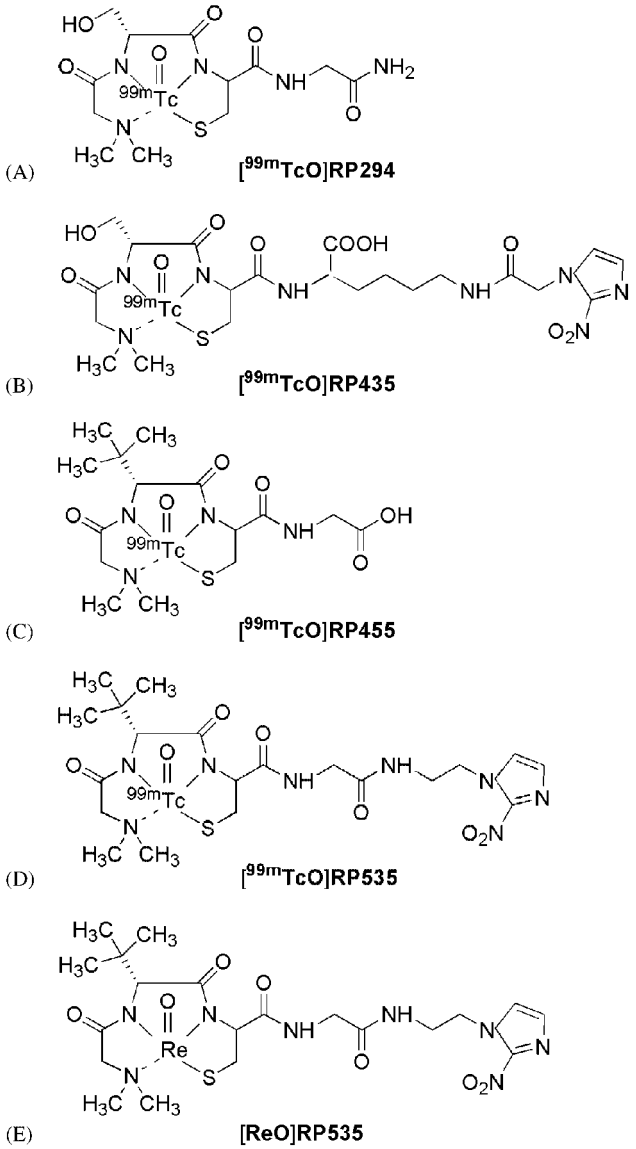


**Figure 1.** Structure of $^{99m}TcO^{3+}$ and $ReO^{3+}$ chelates in *anti* configuration. The structure of $ReO^{3+}$ by RP535 had been confirmed by ES-MS and NMR[22].

dimethylglycyl-L-seryl-L-cysteinyl-lycyl{$N_\varepsilon$-[1-(2-nitro-1*H*-imidazolyl) acetamido]}-glycine (RP435), dimethylglycyl-*tert*-butylglycyl-L-cysteinylglycine (RP455), and dimethylglycyl-*tert*-butylglycyl-L-cysteinylglycine-[2-(2-nitro-1*H*-imidazolyl)ethyl]amide (RP535), were used in this work. When this become clear, [$^{99m}$TcO]$N_3S$ or [$^{186}$ReO]$N_3S$ and [$^{188}$ReO]$N_3S$ chelates with predictable and controllable physicochemical properties in favor of high-quality imaging and therapy of cancers or other human diseases can be prepared.

## Results and discussion

Understanding the relationship of the structure of chelator with the physicochemical properties of $^{99m}$Tc or radioactive Re chelates will be helpful in designing quality imaging and therapeutic agents of cancers. Structurally, an [MO]$N_3S$ chelate exhibits a distorted square pyramidal geometry with the oxo moiety in the apical position, and the orientation of a group on the square plane with respect to the M═O bond will lead to the

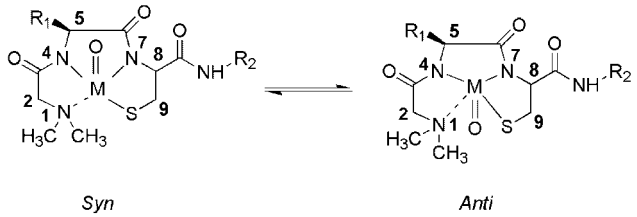


**Figure 2.** [MO]$N_3S$ chelates displayed a distorted square pyramidal geometry with the oxo moiety in the apical position. Theoretically, the up- or under-plane position of the substitutions on C-1, C-2, C-5, C-8, and C-9 can result in the production of *syn* and *anti* isomers of a chelate.

generation of stereoisomers with *syn* and *anti* configurations (Figure 2). Our previous results indicated that the stability of [$^{99m}$TcO]$N_3S$ showed a dependency on media pH values. The chelates were generally stable in acidic solution, but would undergo decomposition in basic and even in neutral solution. This pH dependency may suggest the involvement of an $OH^-$ anion, which functioned to change the stability of the [MO]$N_3S$ chelate through a certain mechanism. Considering the tendency of a $TcO^{3+}$ or a $ReO^{3+}$ ion combining oxygen to return to the stable form of $[MO_4]^-$, it was suspected that the central metal ion was the most likely element in the chelate to react with an $OH^-$ anion. If this was the case, coordination of an $H_2O$ molecule or an $OH^-$ anion to the central metal ion may cause some changes to the chelates in isomers interconversion and stability. According to this hypothesis, interconversion rates and even a specific configuration of an [MO]$N_3S$ chelate can be dominated by properly inhibiting the accessibility of an $H_2O$ molecule or an $OH^-$ anion to the central metal ion. This can be realized by placing groups with appropriate steric hindrance effect at proper positions of a chelator (Figure 2). On the other hand, this hypothesis suggests that the effects such as media pH values, nature of donor atoms, and groups and side-chains on the chelator of an [MO]$N_3S$ compound may be on either facilitating or inhibiting the association of an $H_2O$ or an $OH^-$ with the central metal ion followed by interconversion and/or decomposition of the chelate.

The four $N_3S$ chelators used in this study were RP294, RP435, RP455, and RP535. RP294 and RP435 had the same chelator with a hydroxymethyl group on the C-5 position, while RP455 and RP535 each had a *t*-Bu group on the same position of the chelator backbone. In addition, the side-chains of RP435 and RP535 were conjugated by a hydrophobic 2NI group as a tumor hypoxia selective group, while the side-chains of RP294 and RP455 containing no 2NI group were comparatively short. Similar to the results reported previously,[22] the hydroxymethyl and *t*-Bu groups on these $N_3S$ chelators exhibited influence on the $^{99m}$Tc labeling yields. Although $^{99m}$Tc labeling of both RP294 and RP435 was able to be carried out at room temperature, the radiolabels each presented two interconvertible stereoisomers with combined yields of 97% for [$^{99m}$TcO]RP294 and 69% for [$^{99m}$TcO]RP435, indicating the interference of a larger side-chain on the labeling yield of an $N_3S$ chelator. The HPLC retention time ($R_t$) difference of two isomers of [$^{99m}$TcO]RP294 was 2.0 min, while that of [$^{99m}$TcO]RP435 was 3.2 min (with a deeper HPLC gradient, Figure 3, panels (a) and (b)), again suggesting that the difference of hydrophobicity between these undesignated *syn* and *anti* stereoisomers associated with the size of side-chains. Unlike the hydroxymethyl group on RP294 and RP435, the *t*-Bu group of RP455 and RP535 also interfered with the labeling

Journal of
Labelled Compounds and
Radiopharmaceuticals

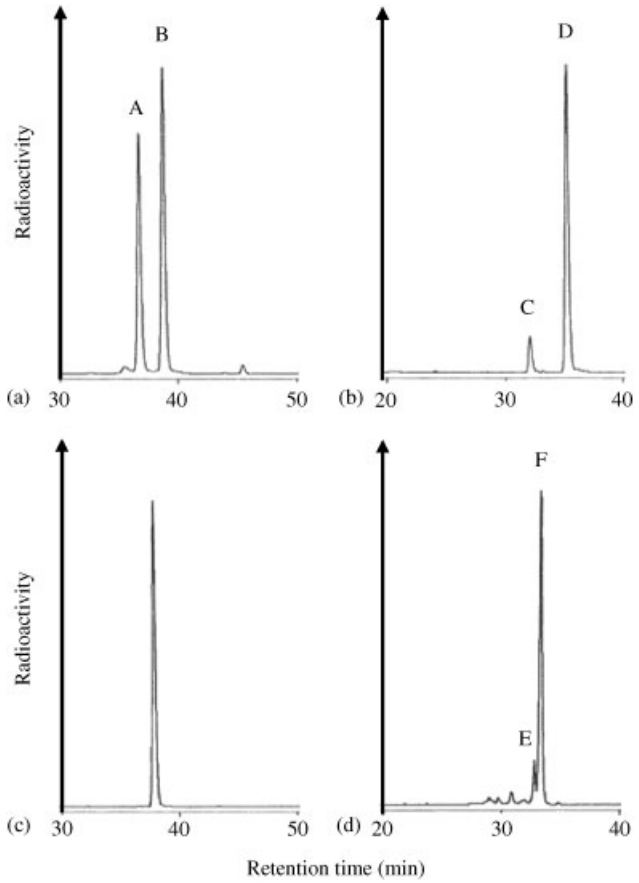


**Figure 3.** HPLC of $^{99m}$Tc labeling of RP294 (peak *A*, $R_t$ = 36.8 min; peak *B*, $R_t$ = 38.8 min) shows a combined yield of 97% (a). Panel (b) shows the evidence of conversion of the purified peak *D* of [$^{99m}$TcO]RP435 into peak *C* after 6.5 h incubation in pH 1.87 aqueous solution. Panel (c) shows the HPLC of $^{99m}$Tc labeling of RP455 ($R_t$ 37.9 min, yield 99%). The labeling of RP535 produced major isomer (peak *F*, $R_t$ 35.4 min, yield ~78%) and a minor component (peak *E*, $R_t$ 32.8, yield ~8%) as is shown on HPLC with a mobile-phase gradient of 100–30% $H_2O$ over 45 min (d).

because improved labeling yields (with 99% for [$^{99m}$TcO]RP455 and 78% for [$^{99m}$TcO]RP535) were achieved only at elevated temperature.[22] Contrary to [$^{99m}$TcO]RP294 and [$^{99m}$TcO]RP435 which exhibited two interconvertible stereoisomers, [$^{99m}$TcO]RP455 presented only one single peak on HPLC (panel (c) of Figure 3), while [$^{99m}$TcO]RP535 showed one major fraction (peak *F*, yield 78%, panel (d) of Figure 3) and a minor one (peak *E*, yield ~8%) nearby. This result clearly indicated that the existence of one or both stereoisomers of an [MO]$N_3$S chelate was determined by the position, orientation, and size of groups on the chelator backbone. Here, a question arises: in the case of [$^{99m}$TcO]RP455, what is the role of the *t*-Bu group in successfully preventing the other isomer from existing in the labeling solution? A simple answer might be that the *t*-Bu group inhibited the coordination of an $H_2O$ molecule or an $OH^-$ anion to the central metal ion at the site opposite to the M═O bond. As indicated by the literature,[23] once a water molecule is associated with the central metal ion, the M═O bond could be switched to the reversed direction through several procedures that caused the conversion of a stereoisomer. Since $TcO^{3+}$ and $ReO^{3+}$ are oxygen attractive ions that have a tendency of combining either oxygen or $H_2O$ or $OH^-$ to return to the stable form of $[MO_4]^-$, it is hypothesized that this tendency may be kept by the central metal ion of an [MO]$N_3$S chelate and is the cause of a stereoisomer converting into the other configuration. If this is true, it is reasonable to designate the observed isomer of [$^{99m}$TcO]RP455 as the isomer in *anti* configuration in which the *t*-Bu group takes a position opposite to the M═O bond. Although both *syn* and *anti* stereoisomers might commonly exist in the labeling solution at the very beginning, the *syn* isomer might have completely converted into the *anti* one, whereas the conversion of an *anti* isomer into the *syn* one was inhibited by the *t*-Bu group, which successfully hindered the association of either an $H_2O$ molecule or an $OH^-$ anion with the central metal ion resulting in the existence of the preferential *anti* isomer. Similarly, the major fraction (peak *F*) of [$^{99m}$TcO]RP535 could be designated as the isomer in *anti* configuration due to the hindrance effect of the *t*-Bu group. The HPLC profiles (Figure 3, panel (a)) demonstrated a 2.0 min retention time difference between peaks *A* and *B* of [$^{99m}$TcO]RP294. The difference in retention times, although small, suggested that peak *A* (with an earlier $R_t$) was more hydrophilic compared with peak *B* (with greater $R_t$). It was suspected that the hydration possibility of the $^{99m}$Tc in a chelate was greater for an isomer with *syn* configuration than that of the *anti* one because the former encountered little hindrance to the hydration of the metal ion. If this is true, peak *A* could be the *syn* isomer while peak *B* the *anti* one. Similar to [$^{99m}$TcO]RP294, [$^{99m}$TcO]RP435 also presented two stereoisomers that were able to undergo interconversion even in a pH 1.87 aqueous solution, as detected by HPLC (Figure 3, panel (b)). Likewise, peak *C* with an earlier retention time might be the isomer in *syn* configuration, and peak *D* the *anti* one. The peaks *C* and *D* displayed a 3.2 min difference between the HPLC retention times, indicating a greater differentiation in hydrophobicity of the *syn* and *anti* isomers compared with peaks *A* and *B* of [$^{99m}$TcO]RP294. As a consequence, the hydrophobicity of an [MO]$N_3$S chelate counted the contribution of the hydrophobicity of its side-chain.

The interconversion of *syn* and *anti* stereoisomers of an [MO]$N_3$S chelate involves the association of a water molecule to the central metal ion,[23] and is facilitated in a aqueous solution with higher pH.[22] In a pH 1.87 aqueous solution, a conversion equilibrium of the *syn* isomer of [$^{99m}$TcO]RP294 into the *anti* one and an *anti* isomer to the *syn* one both took more than 24 h (Figure 4, panel (a)), whereas in Phosphate-buffered saline (PBS) the time required for an equilibrium shortened to 5–30 min (Figure 4, panel (b)). This pH effect became obvious when plotting the panels (a) and (b) together (panels (c) and (d), Figure 4). When incubated in a pH 11.3 aqueous solution for 1 min, both of the isomers of [$^{99m}$TcO]RP294 underwent a complete decomposition into pertechnetate. It was noticed that the conversion of the *syn* isomer of [$^{99m}$TcO]RP294 in either acidic or neutral aqueous solution was always quicker compared with the *anti* one (panels (a) and (b), Figure 4), suggesting the presentation and detectable steric hindrance of the hydroxymethyl group to the hydration of the central metal ion. The pH effects could also be applied to [$^{99m}$TcO]RP435, where the interconversion of its both stereoisomers was quicker in PBS than in pH 1.87 aqueous solution, and it was even quicker in pH 10.8 aqueous solution. Unlike [$^{99m}$TcO]RP294 or [$^{99m}$TcO]RP435, the HPLC-purified [$^{99m}$TcO]RP455 exhibited neither conversion nor change in either acidic or neutral aqueous solutions, signifying the stability of this chelate with *anti* configuration. Similarly, the peak *F* of [$^{99m}$TcO]RP535 was stable in acidic aqueous solution for over 24 h without change, but underwent a



  

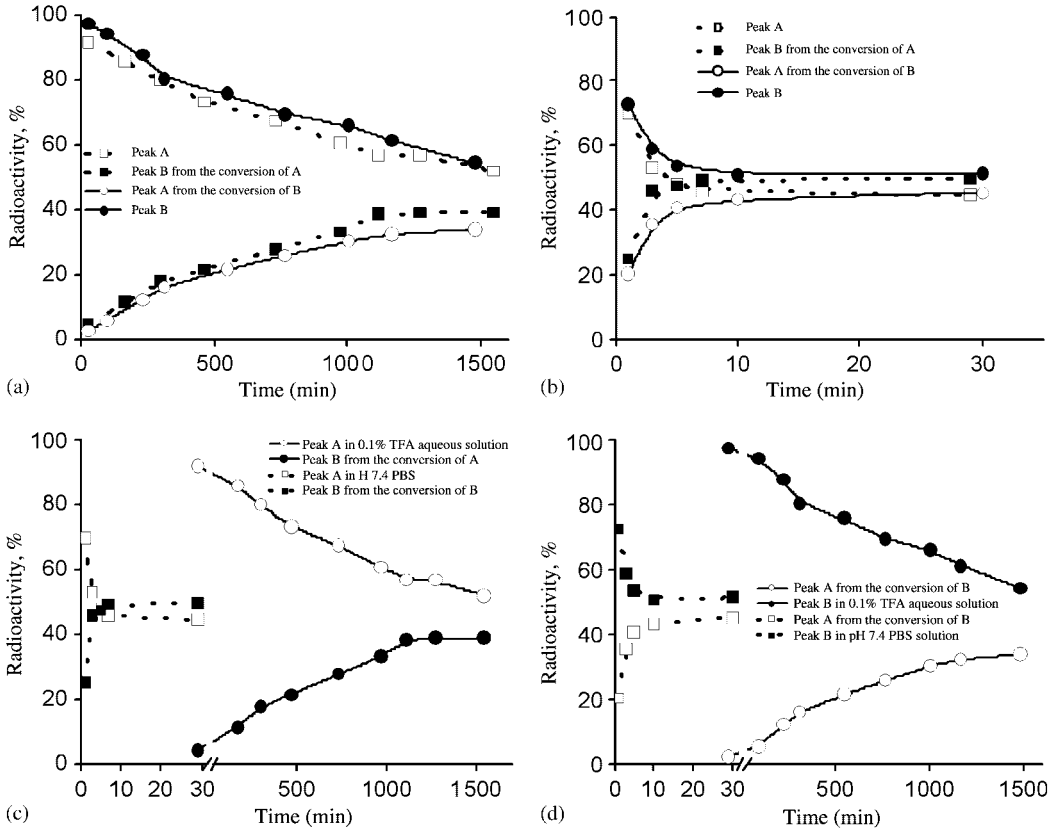


**Figure 4.** Interconversion rate measurement of the two stereoisomers of [$^{99m}$TcO]RP294 (peaks *A* and *B* of Figure 3(a) in pH 1.87 aqueous solution (a) and in pH 7.4 PBS (b). The conversion of the purified peaks *A* into *B* (dotted lines) and the purified *B* into *A* (solid lines) were measured by HPLC, while the percentage of the two isomers against the incubation time was plotted in panels (a) and (b). Panel (c) shows the conversion of peak *A* (incubated in pH 1.87 aqueous solution and pH 7.4 PBS, respectively) into peak *B*, while panel (d) shows the conversion of peak *B* (incubated in the same media, respectively) into peak *A*.

steady decomposition when incubated in 0.25 M PBS and formed three substances showing on HPLC retention times ranging from 22.3 to 23.9 min.[22] As it had previously been indicated that these substances were not the counter isomers of the peak *F*, because they displayed no conversion into the peak *F* when incubated in PBS. The stability difference between [$^{99m}$TcO]RP455 and [$^{99m}$TcO]RP535 suggested that side-chain is also an important factor in determining the stability of chelates. Put together, it is hypothesized that the side-chain and media pH together challenge the hindrance of the *t*-Bu group to enable the hydration of the central metal ion on one hand, and weaken and break down one or several metal–donor atom bonds on the other hand. Although the exact mechanism remains unknown and needs to be proven, the results demonstrate a possibility of controlling the configuration and stability of an [MO]$N_3$S chelate by the combined effects of groups on the backbone of a chelator, side-chains, and medium pH.

For labeling a peptide or a protein with $^{99m}$Tc or radioactive Re, an $N_3$S chelator is often conjugated through its side-chain to the macromolecules.[24–27] In these cases, the macromolecules can be considered as large side-chains that may consequently influence the labeling yields of the conjugates and also the stability of [MO]$N_3$S-peptide or [MO]$N_3$S-protein labels.[28,29] The side-chains of the four chelators used in this work are located on the C-8 carbon which become a chiral carbon atom. Unlike the hydroxymethyl or *t*-Bu groups on the chiral C-5 carbon of the chelators, the orientation of the proton or the side-chain on C-8 with respect to the M═O bond did not present detectable stereoisomers on HPLC chromatograms because the labeling yields of [$^{99m}$TcO]RP294 and [$^{99m}$TcO]RP455 were as great as 97 and 99%, respectively. Why the proton and the flexible side-chain on the C-8 atom did not exhibit detectible stereoisomers of [MO]$N_3$S chelates remains unknown and need to be studied. Even though having the same hydroxymethyl group on C-5 position, both *syn* and *anti* stereoisomers of [$^{99m}$TcO]RP294 always exhibited a faster interconversion rate in either acidic or neutral aqueous solutions than those of [$^{99m}$TcO]RP435, suggesting that a larger side-chain could potentially slow down the interconversion rate of a stereoisomer of [MO]$N_3$S chelates. It was noted that the interconversion equilibrium of the *syn* and *anti* stereoisomers of [$^{99m}$TcO]RP294 and [$^{99m}$TcO]RP435 depended on both media pH and the size of the side-chains. In PBS, the conversion of a *syn* isomer of [$^{99m}$TcO]RP294 to the *anti* one took approximately 5 min to reach an equilibrium, which consisted of 44.6% *syn* isomer and 50.1% *anti* one, whereas the *syn* isomer of [$^{99m}$TcO]RP435 converting into the *anti* configuration required 173 min to reach an equilibrium (containing 42.0% *syn* isomer and 42.8% *anti* one. Figure 5, panel (a)). Similarly, the equilibrium (consisting of 51.5% *anti* isomer and 45.6% *syn* isomer) of the *anti* isomer of [$^{99m}$TcO]RP294 converting to the *syn* one took approximately 30 min to reach, while the conversion of the *anti* isomer of [$^{99m}$TcO]RP435 required 300 min to reach the equilibrium (containing 51.0% *anti* isomer and 47.5 *syn* one, Figure 5, panel (b)). Accordingly, it was suspected that a side-chain might play a role in delaying the conversion of an *anti* isomer through interfering with the

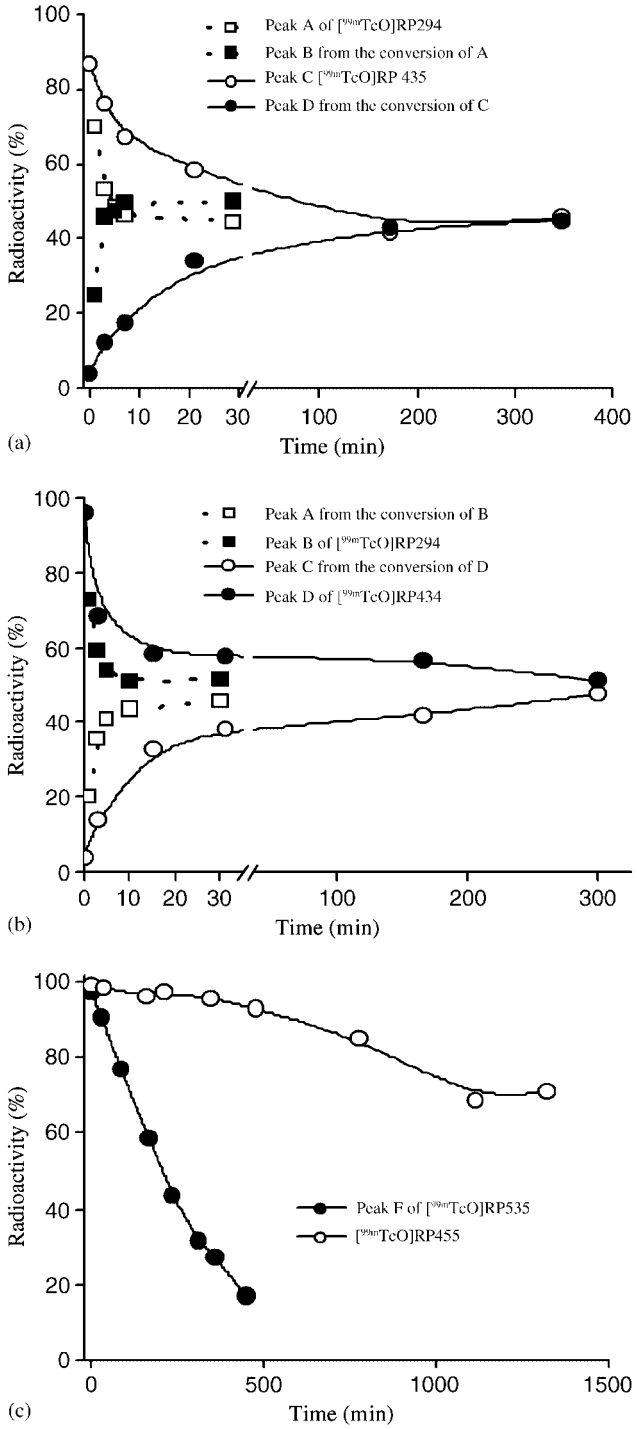


**Figure 5.** The interconversion of peak *A* (dotted line) of [$^{99m}$TcO]RP294 with a shorter side-chain and peak *C* (solid line) of [$^{99m}$TcO]RP435 with a larger side-chain against time is plotted in panel (a), while the conversion of peak *B* (dotted line) of [$^{99m}$TcO]RP294 and peak *D* (solid line) of [$^{99m}$TcO]RP435 against time is plotted in panel (b). When incubating in 0.25 M PBS, the purified [$^{99m}$TcO]RP455 shows a greater stability compared with that of [$^{99m}$TcO]RP535 because the former shows no change for 6 h, while the latter exhibits decomposition along with time and forms substances at $R_t$'s ranging from 22 to 24 min (c).

association of an $H_2O$ molecule or an $OH^-$ anion with the $^{99m}$Tc when it happened to be in the position. In 0.25 M PBS, [$^{99m}$TcO]RP455 did not show significant change for 6 h (Figure 5, panel (c)), while [$^{99m}$TcO]RP535 underwent a steady decomposition forming three substances with greater hydrophilicity ($R_t$'s raging from 22.3 to 23.9 min) compared with the parent molecule ($R_t$ 40.2 min). The three substances were associated with $^{99m}$Tc and were stable in the aqueous solution because they did not undergo a further decomposition into pertechnetate in the time course (Figure 6, panel (a)). Although stable in neutral aqueous solution, [$^{99m}$TcO]RP455 revealed changes and produced two minor substance showing on HPLC with retention times of 11.90 and 35.03 when incubated in pH 11.3 aqueous solution for 2 min (panel (b) of Figure 6). Since the peak at 35.03 min (peak *G*) was close to the parent chelate (peak *H*, $R_t$ 37.28 min) and increased with incubation time of up to 126 min, it was suspected that peak *G* might be the other stereoisomer of [$^{99m}$TcO]RP455. If the peak *H* was the isomer in *anti* configuration because hydration possibility of the central metal ion was diminished by steric hindrance effect of the *t*-Bu on the chelator backbone, the peak *G* must be the isomer in *syn* configuration. The *syn* isomer of [$^{99m}$TcO]RP455 was not detected in the labeling solution possibly because that, if ever existed, it had been completely converted into the *anti* configuration. It needs to be pointed out that in pH 11.3 aqueous solution a severe decomposition of [$^{99m}$TcO]RP455 yielding multiple substances including pertechnetate occurred. By comparison, the peak *E* (yield approximately 8%) of [$^{99m}$TcO]RP535 (Figure 3, panel (d)) could be the stereoisomer in *syn* configuration. This suspicion was supported when the purified peak *E*, which was incubated in 0.25 M PBS and pH 10.8 aqueous solutions, respectively, showed a continuous conversion into the peak *F* (Figure 6, panel (c)). The results demonstrated that at this labeling condition the *syn* isomer of [$^{99m}$TcO]RP455 had been completely converted into the *anti* configuration, while approximately 8% of the *syn* isomer of [$^{99m}$TcO]RP535 remained, implying a delayed conversion of the stereoisomer possibly due to the interference of the side-chain with the hydration of the central metal ion. When incubating in a pH 11.3 aqueous solution, both *syn* and *anti* isomers of [$^{99m}$TcO]RP535 underwent a complete decomposition into pertechnetate suggesting the breakage of all the coordination bonds under this harsh condition. Taken together, the *t*-Bu group had successfully forced the [$^{99m}$TcO]RP455 and [$^{99m}$TcO]RP535 preferentially taking an *anti* configuration, while the decomposition of [$^{99m}$TcO]RP535 in 0.25 M PBS might link to a breakage of one or several coordination bonds caused by the combined effects of $OH^-$, $[H_2PO_4]^-$, $[HPO_4]^{2-}$, and $[PO_4]^{3-}$ ions that squeezed by the *t*-Bu group to coordinate to the $^{99m}$Tc ion, while the side-chain stretched in the direction away from the metal–oxo core. Although this assumption remains unconfirmed, the result revealed a possibility of designing an $[MO]N_3S$ chelate with predictable and controllable stability, configuration and hydrophobicity by properly managing the substituents and side-chains on a chelator to respond the interaction of medium pH.

Contrary to [$^{99m}$TcO]RP535, the *anti* isomer of [ReO]RP535 was stable not only in a pH 11.3 aqueous solution, but also in 0.1 N NaOH solution for over 3 h without any change (Figure 6, panel (d)). This might reflect the significant difference in bond strength and hydration tendency between [$^{99m}$TcO]$N_3S$ and [ReO]$N_3S$ chelates, even though the two metal ions have similar chemical properties such as atomic radius. Since no data about the lengths of the Tc–$N_{amine}$ and Tc–S bonds are available in the literature to make a comparison with that of the Re–$N_{amine}$ and Re–S bonds,[23] it remains unknown whether or not the greater stability of [ReO]RP535 in the alkaline solution over that of [$^{99m}$TcO]RP535 is due to that the former may have stronger

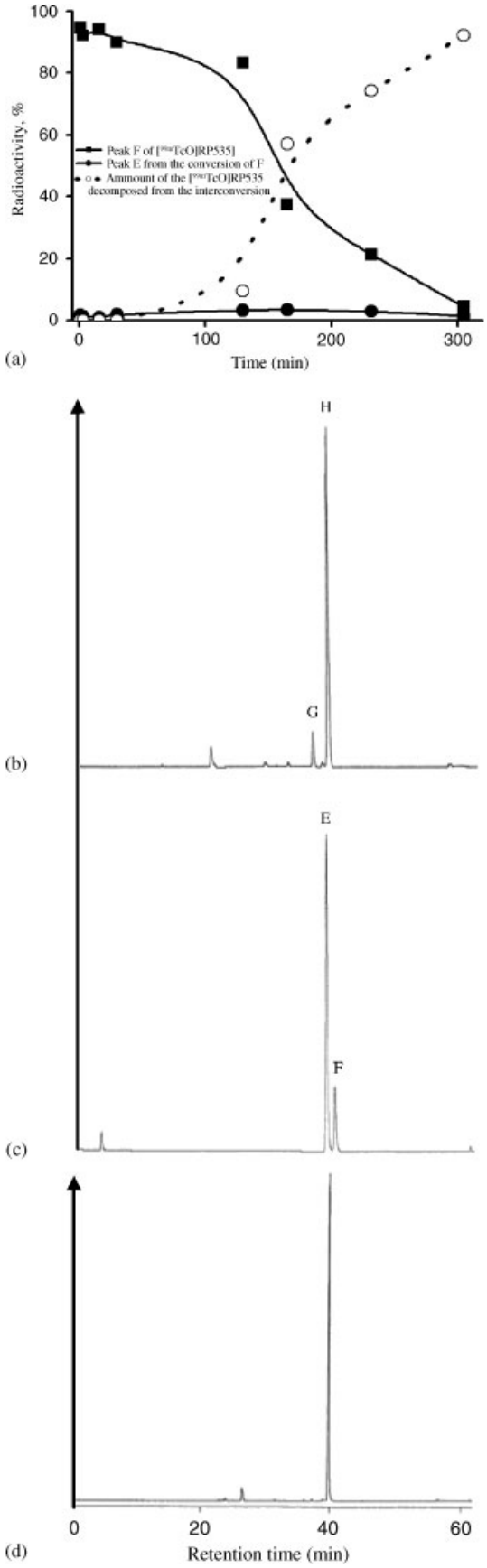


Re–$N_{amine}$ and Re–S bonds compared with those of Tc–$N_{amine}$ and Tc–S. Nevertheless, the results suggested that the coordination bonds of Re–$H_2O$ and Re–OH might be weaker than those of $^{99m}$Tc–$H_2O$ and $^{99m}$Tc–OH and because of this, contrary to [$^{99m}$TcO]RP455 and [$^{99m}$TcO]RP535, in the alkaline aqueous solution neither *syn* isomer coming out from the conversion of the *anti* isomer of [ReO]RP535 nor was decomposition of the chelate seen. Therefore, it can be expected that an [ReO]$N_3$S presents greater stability than the [$^{99m}$TcO]$N_3$S in aqueous solution and, the stereoisomer interconversion rate of the former should be slower than the latter. The difference between [$^{99m}$TcO]$N_3$S and [$^{186}$ReO]$N_3$S and [$^{188}$ReO]$N_3$S in stability added up the variety of physicochemical and pharmacological properties for [MO]$N_3$S chelates.

In addition to the interference with the $^{99m}$Tc labeling and the stability of a chelate as discussed above, the side-chain could contribute its hydrophobicity to the chelate. For example, chromatogram profiles of the *syn* and *anti* isomers of [$^{99m}$TcO]RP435 exhibited greater hydrophobicity (Figures 3, panels (a) and (b)) than those of [$^{99m}$TcO]RP294 for the former had a hydrophobic 2NI group on the side-chain. This signified that the hydrophobicity of a chelate was determined by the hydrophobicity of groups on the chelator backbone and by side-chains. The PC value of the *anti* isomer (peak *F*) of [$^{99m}$TcO]RP535 was $2.8 \pm 0.1$,[22] 127-fold higher than that of [$^{99m}$TcO]RP455 (PC $0.022 \pm 0.001$) and over 2000-fold greater than that of [$^{99m}$TcO]RP435 (PC $0.0010 \pm 0.0001$[22]). This result implied that inhibiting the hydration of the central metal ion might be a more effective approach of increasing the hydrophobicity of a chelate compared with the strategy of conjugating a hydrophobic side-chain to the chelator.

As summarized in Table 1, an [MO]$N_3$S chelate's physicochemical characteristics such as stereoisomerization of the chelate, the stability, conversion rate, and hydrophobicity of the isomers were determined by four factors: the groups on the chelator backbone, the side-chains linked to the chelator, the type of central metal ions, and the medium pH values. Although the hydration of the central metal ion in [MO]$N_3$S can be interfered by the side-chain, the steric hindrance effect of a substituent on the chelator backbone seemed more significant. As shown in Figure 2, an [MO]$N_3$S chelate displayed three five-membered-coordination rings of different sizes, and hetero substitutions on the N-1, C-2, C-8, and C-9 can theoretically produce stereoisomers. Consequently, a group may show different hindrance effect on the hydration of the central metal ion depending on its position on the chelator backbone. According to the data of bond length of the [ReO]RP294 reported in the literature,[23] the perimeters of the three chelation rings (Figure 2) containing N1(amine)–N4(amide)–Re, N4(amide)–N7(amide)–Re, and N7(amide)–S–Re were 8.524, 8.261, and 9.082 Å, respectively. If these bond lengths can be generally applied to other [MO]$N_3$S chelates, it is an assumption that a

**Figure 6.** Panel (a) shows the decomposition of the purified peak *F* of [$^{99m}$TcO]RP535 instead of any interconversion when incubated in a pH 10.8 aqueous solution at room temperature. Panel (b) shows the changes of the preferential [$^{99m}$TcO]RP455 and when incubated in a pH 11.3 aqueous solution for 2 min. Peak *G* grew and peak *H* decreased along with the incubation time, suggesting that peaks *G* and *H* were *syn* and *anti* stereoisomers. Panel (c) exhibits the conversion of the purified peak *E* ($R_t$ 38.9) of [$^{99m}$TcO]RP535 into peak *F* ($R_t$ 40.2 min) when incubated in pH 10.8 aqueous solution for 3 min. The HPLC mobile-phase gradient was 100–50% $H_2O$ over 45 min. Panel (d) shows the stability of [ReO]RP535 after being incubated in 0.1 NaOH aqueous solution for approximately 3.5 h.

**Table 1.** Evaluation of the correlation of some factors with the physicochemical characteristics of a $[MO]N_3S$ chelate

| | Physicochemical characteristics | | | |
|---|---|---|---|---|
| Factors | Labeling yield | Stability | Hindrance of isomers forming in labeling | Conversion rate of isomers |
| Property of backbone substituent | +++[a] | +++ | +++ | +++ |
| Length of side chains | ++ | + | + | ++ |
| Metal ions | + | +++ | + | +++ |
| Media pH | ++ | ++ | + | +++ |

[a]Three plus sign represents a most significant influence.

group on a smaller ring may exert greater hindrance effect to the hydration of central metal ion, while the one on a larger ring may have a weaker effect. If this is true, the *t*-Bu group on the C-2 position may present a smaller steric hindrance effect compared with C-5, whereas the one on the C-9 position will have the weakest effect. This information will be helpful for evaluating and predicting the configuration, stability, and lipophilicity of an $[MO]N_3S$ chelate with bio-reactive or bio-selective groups either substituted on the chelator backbone or conjugated at the side-chain. If the groups are conjugated on side-chains, it may affect the stability of a $[^{99m}TcO]N_3S$ chelate but possibly not an $[^{186}ReO]N_3S$ or an $[^{188}ReO]N_3S$ chelate. If the group is on the chelator backbone, it may affect the stereoisomerization of the $[MO]N_3S$ chelate and the stability of the stereoisomers in aqueous solution. Moreover, the results may lead to designing novel $[MO]N_3S$ chelates with an expectation of showing greater accumulation level in tumor than in normal tissue and in the circulation because the pH value in a tumor is generally lower than that in normal tissue and in the circulation.[30,31] In this situation, an $[MO]N_3S$ chelate may retain longer in tumor than in the circulation where it may undergo more decomposition forming substances with greater hydrophilicity and consequently is cleared from the circulation more quickly.

## Experimental

The preparation, purification, and characterization of the four chelating agents, dimethylglycyl-L-seryl-L-cysteinylglycinamide (RP294), dimethylglycyl-L-seryl-L-cysteinyl-lycyl{$N_\varepsilon$-[1-(2-nitro-1*H*-imidazolyl)acetamido]}-glycine (RP435), dimethylglycyl-*tert*-butylglycyl-L-cysteinylglycine (RP455), dimethylglycyl-*tert*-butyl-glycyl-L-cysteinylglycine-[2-(2-nitro-1*H*-imidazolyl)ethyl]amide (RP535), and [ReO]RP535 were carried out in the established manner reported previously.[22] Radiochemical purity, stability, and the rates of interconversion of the *syn* and *anti* isomers of the $^{99m}$Tc-labeled peptides and [ReO]RP535 (Figure 1) were measured on a Beckman 125 model Gold System (HPLC) with a Zorbax 4.6 × 250 mm 5 μm $C_{18}$ column or Beckman ODS $C_{18}$ 5 μm 4.6 × 250 mm column and UV and radiometric detectors connected in series. The mobile phase consisted of $H_2O$/ACN containing 0.1% trifluoroacetic acid at a flow rate of 1.0 mL/min. The gradients varied from 100% $H_2O$ to 90% $H_2O$ over 45 min for $[^{99m}TcO]$RP294, 100–70% $H_2O$ over 45 min for $[^{99m}TcO]$RP435, 100–50% $H_2O$ over 45 min for $[^{99m}TcO]$RP455, and 100–30% $H_2O$ over 45 min and 100–50% $H_2O$ over 45 min for $[^{99m}TcO]$RP535.

*Techenetium-99m labeling of RP294, RP435, RP455, and RP535*: A peptide with a quantity of 100–200 μg (0.15–0.48 μmol) was mixed with 2–10 mCi $Na^{99m}TcO_4$ in 200 μL of saline. To the mixture was added dropwise 100 μL of an aqueous solution of $SnCl_2$ (40 μL) and sodium gluconate (0.25–1.0 mg). After incubation at room temperature (for RP294 and RP435) or in a boiling water bath (for RP455 and RP535) for 15 min, the labeling mixture was injected into the HPLC for analysis.

*Measurement of the partition coefficient (PC) of $[^{99m}TcO]$RP455 between octanol/PBS*: 10 μL of the HPLC-purified $[^{99m}TcO]$RP455 was added to 1.0 mL of 0.1 M pH 7.4 PBS which was previously saturated with *n*-octanol. The aqueous solution was mixed with 1.0 mL of PBS-saturated *n*-octanol and vortexed for 1 min. After separation of phases, 0.7 mL of each phase was transferred to a microcentrifuge tube and centrifuged at 10 000 *g* for 5 min. The radioactivity in triplicate 0.1 mL aliquots of each phase was counted in a Picker Pace-1 gamma counter (counting time 0.3 min, window 130–150 keV). The partition coefficient (radioactivity in *n*-octanol over that in PBS) was the mean of two parallel tests.

*Measurement of the interconversion rates of stereoisomers of $[^{99m}TcO]$RP294 and $[^{99m}TcO]$RP435*: HPLC-purified peaks *A* and *B* of $[^{99m}TcO]$RP294 (Figure 3, panel (a)) and peaks *C* and *D* of $[^{99m}TcO]$RP435 (Figure 3, panel (b)) were incubated, respectively, in aqueous solution with given pH values for a certain period, and then reinjected into the HPLC for analysis with the same mobile phase and gradients.

*Identification of the syn and anti isomers of $[^{99m}TcO]$RP455 and $[^{99m}TcO]$RP535*: The single peak of $[^{99m}TcO]$RP455 (Figure 3, panel (c)) and the two peaks (peaks *E* and *F*) of $[^{99m}TcO]$RP535 (Figure 3, panel (d)) were collected. The purified fractions were incubated, respectively, in the pH 1.87 aqueous solution, PBS, pH 10.8, and pH 11.3 aqueous solution for a given time interval, and then reinjected into HPLC with the same mobile phases and gradients.

## Conclusion

Like $[MO]N_2S_2$ and $[MO]N_4$ chelates (where M represents $^{99m}$Tc, $^{99}$Tc, Re, $^{186}$Re, and $^{188}$Re), an $[MO]N_3S$ chelate exhibit a distorted square pyramid geometry with the M═O bond in apical position, while the orientation of hetero substitutions on the chelator backbone with respect to the M═O bond will theoretically result in the production of *syn* and *anti* stereoisomers. The interconversion of the stereoisomers involves the association of an $H_2O$ molecule with the central metal ion and is facilitated by elevated pH. Therefore, the interconversion rates of the stereoisomers of a $[MO]N_3S$ chelate may possibly be dominated through controlling the hydration possibility/feasibility of the central metal ions. The substitutions on the chelator's backbone may exhibit more or less steric hindrance effects to the association of an $H_2O$ or an $OH^-$ anion to the

metal ion. The hydroxymethyl of [$^{99m}$TcO]RP294 and [$^{99m}$TcO]RP435 is a minor steric hindrant and hence displays a weak interference with the interconversion of the *syn* and *anti* isomers of the chelates, while *t*-Bu of [$^{99m}$TcO]RP455 and [$^{99m}$TcO]RP535 presents significant interference with the interconversion of the stereoisomers and also make the chelates taking preferential *anti* configurations. Side-chains will not only contribute their hydrophobicity to the chelates, but also control the interconversion rates of stereoisomers of a chelate as shown by [$^{99m}$TcO]RP435 and [$^{99m}$TcO]RP294. In the case of [$^{99m}$TcO]RP455 and [$^{99m}$TcO]RP535, the former was stable in neutral aqueous solution while the latter underwent a steady decomposition possibly due to its larger side-chain interfering with the stability. Contrarily, [ReO]RP535 exhibited stability in both neutral aqueous solution and 0.1 N NaOH, suggesting stronger coordination bonds of the chelate compared with those of [$^{99m}$TcO]RP535 and implying a difference of hydration tendency between $^{99m}$Tc and Re. Therefore, it can be expected that [$^{99m}$TcO]$N_3S$, [$^{186}$ReO]$N_3S$, and [$^{188}$ReO]$N_3S$ display significant differences in interconversion rate and stability in aqueous solutions. Taken together, a [MO]$N_3S$ chelate with controllable and predictable configuration, stability, and lipophilicity can be designed and prepared through strategies of managing (1) one or more proper substituents on appropriate position of the chelator backbone, (2) a proper side-chain, and (3) a proper radioactive central metal ion to respond the influence of medium pH.

## Acknowledgements

Z. S. is grateful to Drs James R. Ballinger (Guy's and St Thomas' Hospital, London, UK) and A. M. Rauth (Division of Experimental Therapeutics, Ontario Cancer Institute, Toronto, Ontario, Canada) for the kind and generous help with this work.

## References

[1] C. G. Van Nerom, G. M. Bormans, M. J. De Roo, A. M. Verbruggen, *Eur. J. Nucl. Med.* **1993**, *20*, 738–746.
[2] J. K. Moran, *Semin. Nucl. Med.* **1999**, *29*, 91–101.
[3] F. P. Esteves, A. Taylor, A. Manatunga, R. D. Folks, M. Krishnan, E. V. Garcia, *AJR Am. J. Roentgenol.* **2006**, *187*, W610–W617.
[4] Y. Kohn, N. Freedman, H. Lester, Y. Krausz, R. Chisin, B. Lerer, O. Bonne, *J. Nucl. Med.* **2007**, *48*, 1273–1278.
[5] M. A. Ansar, Y. Osaki, H. Kazui, N. Oku, M. Takasawa, Y. Kimura, N. N. Begum, Y. Ikejiri, M. Takeda, J. Hatazawa, *Ann. Nucl. Med.* **2006**, *20*, 511–517.
[6] S. Vallabhajosula, R. E. Zimmerman, M. Picard, P. Stritzke, I. Mena, R. S. Hellman, R. S. Tikofsky, M. G. Stabin, R. A. Morgan, S. J. Goldsmith, *J. Nucl. Med.* **1989**, *30*, 599–604.
[7] E. Guedj, D. Taieb, S. Cammilleri, D. Lussato, C. de Laforte, J. Niboyet, O. Mundler, *Eur. J. Nucl. Med. Mol. Imaging* **2007**, *34*, 130–134.
[8] H. Kusuoka, K. Hashimoto, K. Fukuchi, T. Nishimura, *J. Nucl. Med.* **1994**, *35*, 1371–1376.
[9] J. R. Ballinger, J. W. Kee, A. M. Rauth, *J. Nucl. Med.* **1996**, *37*, 1023–1031.
[10] T. Melo, J. Duncan, J. R. Ballinger, A. M. Rauth, *J. Nucl. Med.* **2000**, *41*, 169–176.
[11] S. K. Meegalla, K. Plossl, M. P. Kung, S. Chumpradit, D. A. Stevenson, S. A. Kushner, W. T. McElgin, P. D. Mozley, H. F. Kung, *J. Med. Chem.* **1997**, *40*, 9–17.
[12] K. O. Mang'era, H. P. Vanbilloen, C. W. Schiepers, A, M. Verbruggen, *Eur. J. Nucl. Med.* **1995**, *22*, 1163–1172.
[13] X. Zhang, T. Melo, J. R. Ballinger, A. M. Rauth, *Int. J. Radiat. Oncol. Biol. Phys.* **1998**, *42*, 737–740.
[14] D. Stepniak-Biniakiewicz, B. H. Chen, E. Deutsch, *J. Med. Chem.* **1992**, *35*, 274–279.
[15] H. F. Kung, B. L. Liu, Y. Wei, S. Pan, *Int. J. Radiat. Appl. Instrum. [A]* **1990**, *41*, 773–781.
[16] J. R. Dilworth, S. J. Parrott, *Chem. Soc. Rev.* **1998**, *27*, 43–55.
[17] D. Eshima, A. Taylor Jr, A. R. Fritzberg, S. Kasina, L. Hansen, J. F. Sorenson, *J. Nucl. Med.* **1987**, *28*, 1180–1186.
[18] K. Ogawa, T. Mukai, Y. Arano, M. Ono, H. Hanaoka, S. Ishino, K. Hashimoto, H. Nishimura, H. Saji, *Bioconjug. Chem.* **2005**, *16*, 751–757.
[19] S. Kasina, J. A. Sanderson, J. N. Fitzner, A. Srinivasan, T. N. Rao, L. J. Hobson, J. M. Reno, D. B. Axworthy, P. L. Beaumier, A. R. Fritzberg, *Bioconjug. Chem.* **1998**, *9*, 108–117.
[20] C. S. Hilger, M. C. Willis, M. Wolters, W. A. Pieken, *Nucleos. Nucleot.* **1999**, *18*, 1479–1481.
[21] F. Chang, M. Rusckowski, T. Qu, D. J. Hnatowich, *Cancer* **1997**, *80*(12 Suppl.), 2347–2353.
[22] Z. F. Su, X. Zhang, J. R. Ballinger, R. A. Rauth, A. Pollak, J. R. Thornback, *Bioconjug. Chem.* **1999**, *10*, 897–904.
[23] E. Wong, T. Fauconnier, S. Bennett, J. Valliant, T. Nguyen, F. Lau, L. F. L. Lu, A. Pollak, R. A. Bell, J. R. Thornback, *Inorg. Chem.* **1997**, *36*, 5799–5808.
[24] Y. R. Zhang, Y. X. Zhang, W. Cao, X. L. Lan, *J. Nucl. Med.* **2005**, *46*, 1052–1058.
[25] S. Kasina, J. A. Sanderson, J. N. Fitzner, A. Srinivasan, T. N. Rao, L. J. Hobson, J. M. Reno, D. B. Axworthy, P. L. Beaumier, A. R. Fritzberg, *Bioconjug. Chem.* **1998**, *9*, 108–117.
[26] C. S. Hilger, M. C. Willis, M. Wolters, W. A. Pieken, *Nucleos. Nucleot.* **1999**, *18*, 1479–1481.
[27] C. J. Smith, H. Gali, G. L. Sieckman, C. Higginbotham, W. A. Volkert, T. J. Hoffman, *Bioconjug. Chem.* **2003**, *4*, 93–102.
[28] L. Gano, L. Patricio, E. Marques, G. Cantinho, H. Pena, T. Martins, D. J. Hnatowich, *Nucl. Med. Biol.* **1998**, *5*, 395–403.
[29] D. J. Hnatowich, T. Qu, F. Chang, A. C. Ley, R. C. Ladner, M. Rusckowski, *J. Nucl. Med.* **1999**, *39*, 56–64.
[30] K. Glunde, S. E. Guggino, M. Solaiyappan, A. P. Pathak, Y. Ichikawa, Z. M. Bhujwalla, *Neoplasia* **2003**, *5*, 533–545.
[31] B. P. Mahoney, N. Raghunand, B. Baggett, R. J. Gillies, *Biochem Pharmacol* **2003**, *66*, 1207–1218.